RSC Advances

PAPER

View Article Online
View Journal | View Issue

Cite this: *RSC Adv.*, 2023, **13**, 16369

Synthesis and photophysical characterization of fluorescent indole nucleoside analogues†

Jacob M. Sawyer,[a] Kellan T. Passow[b] and Daniel A. Harki *[ab]

Received 23rd May 2023
Accepted 25th May 2023

DOI: 10.1039/d3ra03457g

rsc.li/rsc-advances

Fluorescent nucleosides are useful chemical tools for biochemical research and are frequently incorporated into nucleic acids for a variety of applications. The most widely utilized fluorescent nucleoside is 2-aminopurine-2′-deoxyribonucleoside (**2APN**). However, **2APN** is limited by a moderate Stokes shift, molar extinction coefficient, and quantum yield. We recently reported 4-cyanoindole-2′-deoxyribonucleoside (**4CIN**), which offers superior photophysical characteristics in comparison to **2APN**. To further improve upon **4CIN**, a focused library of additional analogues combining the structural features of **2APN** and **4CIN** were synthesized and their photophysical properties were quantified. Nucleosides **2**–**6** were found to possess diverse photophysical properties with some features superior to **4CIN**. In addition, the structure–function relationship data gained from **1**–**6** can inform the design of next-generation fluorescent indole nucleosides.

Introduction

Isomorphic fluorescent nucleosides are structurally similar to naturally occurring nucleosides and aim to retain the intra- and inter-molecular interactions found with endogenous nucleosides and other molecules. 2-Aminopurine-2′-deoxyribonucleoside (**2APN**) is the most widely utilized isomorphic fluorescent nucleoside because of its environment sensitive fluorescence along with only minor perturbations to the native B-form DNA structure, which results in only a slight reduction in overall stability of duplex DNA.[1–4] Despite its widespread use, **2APN** has significant limitations in terms of its photophysical properties such as a moderate Stokes shift, molar extinction coefficient, and quantum yield. The development of fluorescent nucleoside analogues that improve upon the photophysical properties of **2APN** has been an area of significant research interest.[5–7] Recently, 4-cyanoindole (**4CI**) was developed into the corresponding fluorescent nucleoside 4-cyanoindole-2′-deoxyribonucleoside (**4CIN**), which is superior to **2APN** in all the aforementioned photophysical properties.[8] **4CI** has been incorporated into a ribonucleoside (**4CINr**) and a 2′-deoxyribonucleoside-2′-triphosphate (**4CINTP**),[9] and **4CIN** has served as a useful probe for DNA[8,10] and RNA applications.[11] To further optimize **4CIN** and interrogate the scope of structural modifications that can contribute to favorable photophysical properties, a library of fluorescent nucleosides combining the structural features of **4CIN** and **2APN** were synthesized and their photophysical properties characterized (Fig. 1). Nucleoside **1** contains the classical purine heterocycle with the introduction of a nitrile at the 6-position, which is analogous to the 4-position on indole. Nucleoside **2** interrogates whether a 6-amino group can be installed on the 4-cyanoindole (**4CI**) heterocycle and retain fluorescence properties. In addition, **2** incorporates the amino group found in guanosine, which may be useful in applications involving duplex DNA. Nucleosides **3** and **4** interrogate conversion of the nitrile of **2** to an ester and acid (**3** and **4**, respectively), whereas **5** and **6** continue that line of investigation to determine if the pendant 6-amino group contributes to

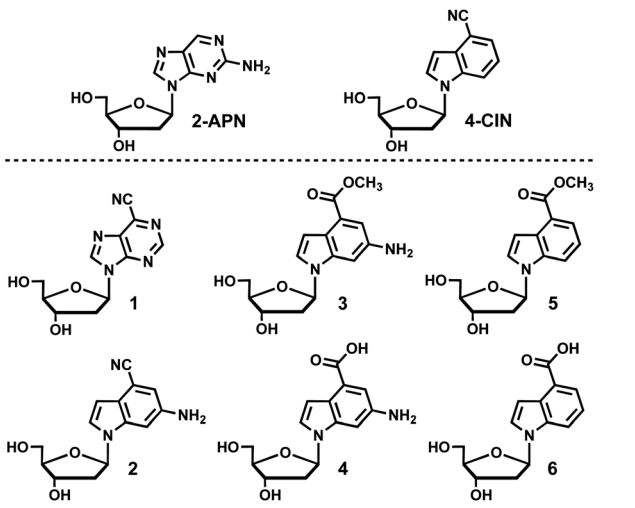

Fig. 1 A library of fluorescent nucleosides (**1**–**6**) combining the structural features of **2APN** and **4CIN**.

[a]*Department of Chemistry, University of Minnesota, Minneapolis, Minnesota 55455, USA. E-mail: daharki@umn.edu*

[b]*Department of Medicinal Chemistry, University of Minnesota, Minneapolis, Minnesota 55455, USA*

† Electronic supplementary information (ESI) available. See DOI: https://doi.org/10.1039/d3ra03457g

favorable photophysical properties. Interestingly, we find that **5** and **6** have higher molar extinction coefficients than **2APN** and **4CIN**, as well as a higher quantum yield than **2APN**.

Results and discussion

Synthesis

The synthesis of 6-cyanopurine-2′-deoxyribonucleoside **1** began with silyl protection of the 3′- and 5′-hydroxyls of 6-chloropurine-2′-deoxyribonucleoside **7** to yield **8**. The nitrile was then installed at the 6-position using a palladium-catalyzed cyanation reaction with zinc cyanide to afford **9** in good yield.[12] Deprotection of the silyl groups afforded **1** in 36% overall yield (Scheme 1).

6-Amino-4-cyanoindole-2′-deoxyribonucleoside (**2**) was prepared from 6-amino-4-cyanoindole (**10**) (Scheme 2). Dibenzyl protection of the exocyclic amine of **10** resulted in **11** in moderate yield, which provided the coupling partner for established chlorosugar **12** to afford **13** as the β-anomer in good yield. Removal of the *N*-benzyl and *O*-toluoyl protecting groups in a 2-step process afforded **2** in an overall yield of 8%.

To synthesize the nucleosides bearing 6-amino-4-carboxyindoles (**3** and **4**) we started with dinitro-toluic acid (**15**), which underwent a Fischer esterification to generate the carboxylate ester (**16**, Scheme 3). Ester **16** was then subjected to Leimgruber–Batcho indole synthesis conditions to afford **17**.[13,14] The subsequent 4 synthesis steps were analogous to those described for the preparation of **2**, including benzyl protection of the exocyclic amine of **17**, coupling of indole **18** to chlorosugar **12**, benzyl deprotection of **19**, and saponification of the toluoyl esters of **20** to produce **3** in 6% overall yield. Treatment of **20** directly with aqueous KOH saponified the methyl carboxylate and toluoyl groups yielding **4**. However, we wanted to access the methyl carboxylate compound for photophysical testing so this conversion was done over two steps. Employing a weaker base than hydroxide allowed selective removal of the toluoyl groups while avoiding hydrolysis of the methyl carboxylate. Carboxylic acid **4** was then synthesized from **3** by ester saponification with aqueous KOH in 43% yield.

To access 4-carboxyindole analogues **5** and **6**, a simpler synthesis was employed as these indoles lack the exocyclic amine (Scheme 4). Indole **21** was coupled directly to chlorosugar **12** followed by deprotection of the toluoyl groups to yield **5** with an overall yield of 47%. When treated with aqueous KOH, **5** was smoothly converted to the carboxylic acid analogue **6** in 46% yield.

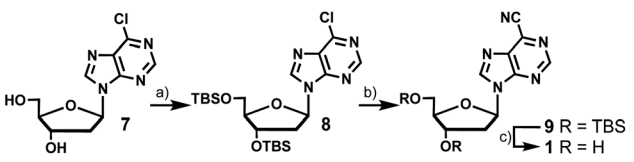

Scheme 1 Synthesis of 6-cyanopurine-2′-deoxyribonucleoside (**1**). Reagents and conditions: (a) TBSCl, imidazole, DMAP, DMF, RT (room temperature) 75%; (b) $Zn(CN)_2$, $Pd(PPh_3)_4$, DMF, 90 °C, 71%; (c) TBAF, THF, RT, 67%.

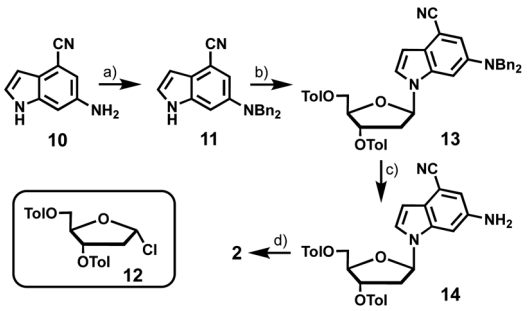

Scheme 2 Synthesis of 4-cyano-6-aminoindole-2′-deoxyribonucleoside (**2**). Reagents and conditions: (a) BnCl, K_2CO_3, MeOH, reflux, 61%; (b) NaH, MeCN, 30 min, RT; **12**, RT, 65%; (c) Pd/C, H_2, THF, RT, 38%; (d) K_2CO_3, MeOH, THF, RT, 50%.

Photophysical characterization of fluorescent nucleosides

The library of fluorescent nucleosides was first characterized by measuring absorption and emission properties (Fig. 2). The nucleosides displayed red-shifted absorption and emission maxima wavelengths in comparison to **2APN** and **4CIN**, granting high Stokes shifts for each of the analogues with the exception of **1** (Table 1). 4-Cyanopurine-2′-deoxyribonucleoside (**1**), built on the purine scaffold, was not a fluorescent compound. For this reason, the nucleoside was excluded from further studies. For the compounds with two absorption maxima (**2**, **3**, and **4**), the photophysical properties were determined using the wavelength with the highest absorption (represented by λ_{ex} in Table 1). **2** contains the 4-cyano group of **4CIN** and the 6-amino group of **2APN**. This compound has a Stokes shift in-between **4CIN** (8.5×10^3 cm^{-1}) and **2APN** (5.9×10^3 cm^{-1}) at 6.9×10^3 cm^{-1}. Analogues **3** and **4** replace the nitrile at the 4-position with a methyl carboxylate ester (**3**) and carboxylic acid (**4**). These functional group changes increased the Stokes shift of both compounds in comparison to **2** granting a Stokes shift of 9.0×10^3 cm^{-1} and 12.9×10^3 cm^{-1} for **3** and **4**, respectively. Nucleosides **5** and **6** are analogous to **3** and **4**, except they lack the 6-amino group. Interestingly, **5** displays a higher Stokes shift than **3** at 10.1×10^3 cm^{-1}. However, in the

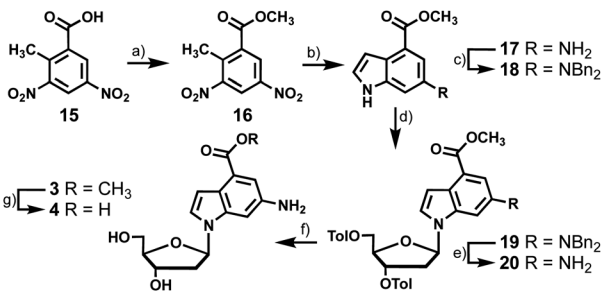

Scheme 3 Synthesis of fluorescent nucleosides with 6-amino and 4-carboxylate ester (**3**) and acid (**4**) substituents. Reagents and conditions: (a) H_2SO_4, MeOH, reflux, 98%; (b) DMF-DMA, dioxane, microwave, 90 °C; H_2, Pd/C, MeOH, RT, 62%; (c) BnCl, K_2CO_3, MeOH, reflux, 54%; (d) NaH, MeCN, 30 min, RT; **12**, RT, 64%; (e) Pd/C, H_2, THF, RT, 55%; (f) K_2CO_3, MeOH, THF, RT, 51%; (g) KOH, MeOH, THF, 50 °C, 43%.

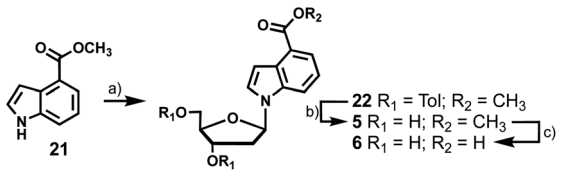

Scheme 4 Synthesis of fluorescent indole nucleosides with 4-carboxylate ester (**5**) and acid (**6**) substituents. Reagents and conditions: (a) NaH, MeCN, 30 min, RT; **12**, RT, 69%; (b) K_2CO_3, MeOH, THF, RT, 68%; (c) KOH, MeOH, THF, H_2O, 50 °C, 46%.

case of **6**, removal of the 6-amino group lowered its Stokes shift in comparison to **4** with a value of 10.1×10^3 cm^{-1}. These data show that the presence of an electron-donating group at the 6-position does not clearly correlate with an effect on the Stokes shift. Regardless, nucleosides **2–6** all have a higher Stokes shift than **2APN** and, with the exception of **2**, a higher Stokes shift than **4CIN**.

The molar extinction coefficients (ε) of nucleosides **2–6** were determined using Beer's law (Table 1). Following the same trend as was seen with the Stokes shift, **2** has a molar extinction coefficient in between that of **2APN** and **4CIN** at 6430 ± 70 M^{-1} cm^{-1}. Changing the functional group at the 4-position from a nitrile to a methyl carboxylate ester increased the molar extinction coefficient of **3** to 7570 ± 100 M^{-1} cm^{-1}. However, converting the functional group at the 4-position to the carboxylic acid had a detrimental effect on the extinction coefficient, reducing the value for **4** to 2780 ± 110 M^{-1} cm^{-1}. Nucleosides **5** and **6** both showed an increase in molar extinction coefficients in comparison to **3** and **4** at 8910 ± 70 M^{-1} cm^{-1} and 8090 ± 50 M^{-1} cm^{-1}, respectively. The molar extinction coefficient for all nucleosides, with the exception of **4**, were higher than **2APN**. **5** and **6** also had higher molar extinction coefficients than **4CIN**. These data show that removing the amine at the 6 position grants an increase in the molar extinction coefficient for the fluorophores.

The quantum yield was next determined for **2–6** (Table 1) using an established method relative to a known standard, quinine sulfate (QS).[18] Breaking from the trend seen for the previous photophysical properties, **2** did not display a quantum yield in between **2APN** and **4CIN**, but a lower quantum yield than both at 0.0067 ± 0.0006. Changing from the 4-cyano to the methyl carboxylate ester granted a significant increase in quantum yield for **3** at 0.083 ± 0.001. Converting to the carboxylic acid increased the quantum yield to 0.53 ± 0.01 for **4**.

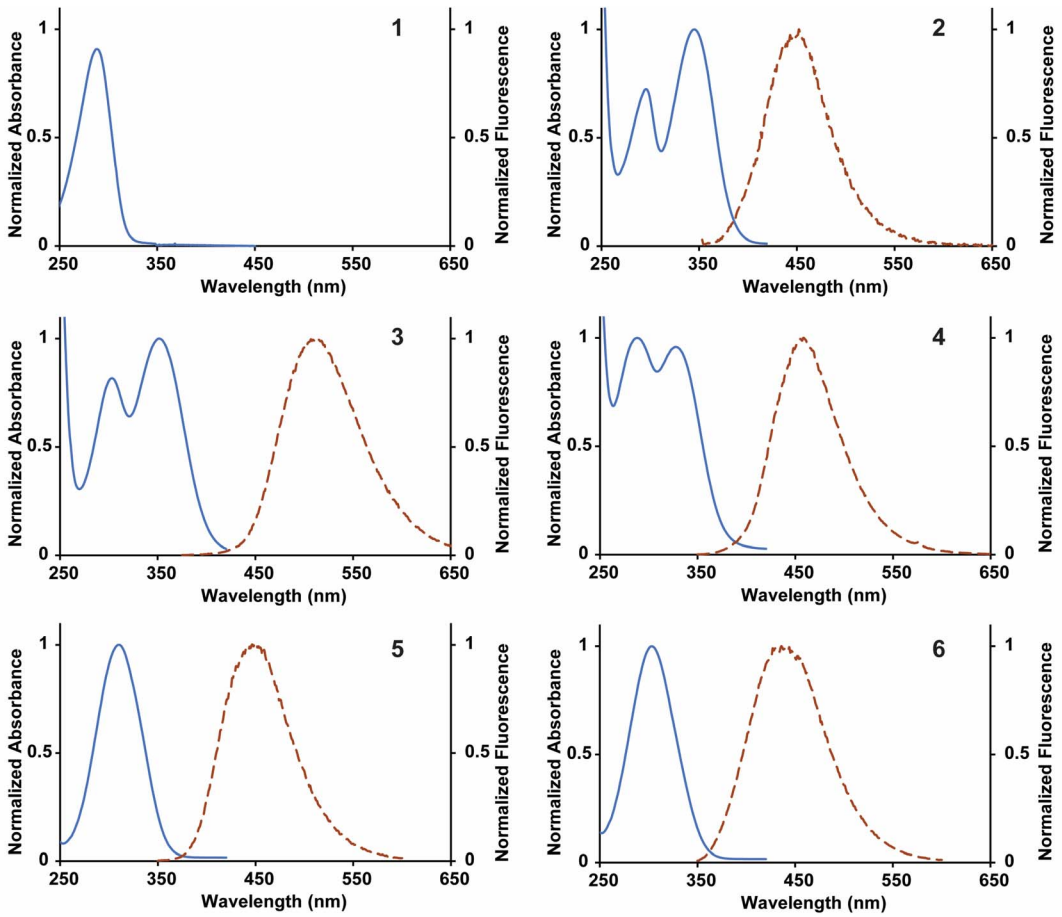

Fig. 2 Normalized absorbance and fluorescence spectra for **1–6** collected in distilled and deionized H_2O. Fluorescence measurements were obtained by exciting the compounds at their absorbance maximum.

Table 1 Photophysical characteristics for the library of fluorescent nucleosides. Published values for **4CIN** and **2APN** are included in the table for reference[8]

Nucleoside	λ_{ex} (nm)	λ_{em} (nm)	Stokes shift (cm^{-1})	ε (M^{-1} cm^{-1})	QY[b]	Brightness[c]
2APN	303	369	5.9×10^3	5000–6000[a]	0.61 ± 0.01	3050–3660
4CIN	305	412	8.5×10^3	7790 ± 320	0.92 ± 0.02	7160
2	296, 345	452	6.9×10^3	6430 ± 70	0.0067 ± 0.0006	40
3	303, 351	514	9.0×10^3	7570 ± 100	0.083 ± 0.001	630
4	288, 327	457	12.9×10^3	2780 ± 110	0.53 ± 0.01	1470
5	310	451	10.1×10^3	8910 ± 70	0.64 ± 0.01	5700
6	303	436	10.1×10^3	8090 ± 50	0.84 ± 0.01	6800

[a] Literature values for **2APN** molar extinction coefficient vary.[15–17] [b] Calculated relative to QS in aqueous 0.105 M $HClO_4$. [c] Brightness was calculated by multiplying ε and QY.

The absence of the amine at the 6-position gave the highest quantum yields of the analogues for **5** and **6** at 0.64 ± 0.01 and 0.84 ± 0.01, respectively, which are both higher than **2APN**. Analysis of quantum yield follows the same trend as the molar extinction coefficient, whereas removal of the 6-amino group is beneficial.

A useful characteristic for the analysis of fluorophores is the brightness (Φ) because it accounts for both the absorption and fluorescence properties of the fluorophore. Due to significant differences in the quantum yield of analogues **2–6** there was a wide range of corresponding brightness values. Nucleosides **2–4** displayed low brightness values owing to either low quantum yields (**2** and **3**) or a low extinction coefficient (**4**). Analogues **5** and **6**, which lack the 6-amino substituent, had significantly higher brightness values than **2APN**. However, **4CIN** still shows the highest brightness of the group.

Conclusions

This study served to combine the structural properties of **4CIN** and **2APN** into a focused library of fluorescent nucleosides with the goal of identifying compounds with improved photophysical properties and further defining structure–function relationships. Six nucleosides were synthesized and characterized photophysically, and then benchmarked against **2APN** and **4CIN**. Nucleoside **1**, which was built upon the purine scaffold, was not a fluorescent compound. This initial result informed our decision to focus on the indole scaffold. The fluorescent nucleosides bearing the 6-amino substituent (**2**, **3**, and **4**) had high Stokes shifts, but overall low brightness. In the case of **2** and **3**, the low brightness is attributed to a low quantum yield. Interestingly, for nucleoside **4**, the low brightness was due to a low molar extinction coefficient. Conversely, the fluorescent nucleosides lacking the 6-amino substituent, **5** and **6**, showed higher Stokes shifts, molar extinction coefficients, and quantum yields in comparison to **2APN**. These compounds also had larger Stokes shifts and molar extinction coefficients than **4CIN**, although **4CIN** has a higher quantum yield. The brightness of **5** and **6** were higher than **2APN**, but not **4CIN**. Taken together, nucleosides **5** and **6** have improved photophysical properties over **2APN** and are viable isomorphic fluorescent nucleosides suitable for future studies. In addition, our data suggest that the presence of an electron donating group at the 6-position of the indole lowers the brightness of fluorescent indole nucleosides, which should inform the design of next-generation compounds with enhanced photophysical properties.

Experimental

General information

Reactions were performed in flame-dried glassware under inert atmospheres (nitrogen or argon). Reactions were stirred using Teflon-coated stir bars. Solvents MeCN and CH_2Cl_2 were dried using an MBraun solvent purification system. Other solvents were purchased as ACS grade (≥99% purity) and used as received. Water for reactions and for photophysical characterization of the fluorescent nucleosides was purified using a MilliQ system (MilliporeSigma). 3,5-Di-*O*-toluoyl-α-1-chloro-2-deoxy-D-ribofuranose (**12**) was purchased from Carbosynth. Microwave reactions were performed on a Discover SP Microwave Synthesizer (CEM Corporation). Conditions used for microwave reactions were as follows: 17 bar, 200 watts, and 90 °C with stirring. Silica gel chromatography was performed using Redisep Rf high performance silica gel columns (Teledyne-Isco) on a Combiflash NextGen 300+ instrument (Teledyne-Isco). A Bruker Advance 500 MHz NMR spectrometer was used for the collection of all NMR spectra. NMR spectra were collected at room temperature. High resolution mass spectrometry was performed at the Analytical Biochemistry Core Facility at the University of Minnesota Masonic Cancer Center on an Exactive Plus Orbitrap mass spectrometer (Thermo Scientific).

Synthesis

3′,5′-Di-*O*-*tert*-butyldimethylsilyl-6-chloropurine-2′-deoxyribonucleoside (8). 6-Chloropurine-2′-deoxyribonucleoside **7** (0.500 g, 1.85 mmol, 1 eq.), TBSCl (0.690 g, 4.58 mmol, 2.5 eq.), imidazole (0.760 g, 11.2 mmol, 6 eq.), DMAP (34.0 mg, 0.278 mmol, 0.15 eq.) were dissolved in anhydrous DMF (15 mL) and stirred under N_2 for 18 hours. The reaction was quenched with the addition of saturated bicarbonate solution (5 mL), extracted into dichloromethane (DCM, 50 mL), washed with

H_2O (40 mL), brine (50 mL), the organic layer dried over Na_2SO_4, and concentrated *in vacuo*. The residue was purified by chromatography on silica gel with a gradient 0–3% MeOH in DCM to yield **8** (0.680 g, 75% yield).

^{1}H NMR ($CDCl_3$, 500 MHz): 8.74 (s, 1H), 8.48 (s, 1H), 6.52 (app t, J = 6.4 Hz, 1H), 4.62 (m, 1H), 4.05 (app q, J = 3.3 Hz, 1H), 3.89 (dd, J = 11.3, 3.7 Hz, 1H), 3.78 (dd, J = 11.3, 2.8 Hz, 1H), 2.64 (m, 1H), 2.49 (m, 1H), 0.92 (s, 9H), 0.90 (s, 9H), 0.11 (s, 6H), 0.09 (s, 6H) δ ppm.

^{13}C NMR ($CDCl_3$, 126 MHz): 151.9, 151.1, 151.0, 143.8, 132.2, 88.2, 84.9, 71.8, 62.7, 41.6, 26.0, 25.7, 18.4, 18.0, −4.6, −4.8, −5.4, −5.5 δ ppm.

HRMS-ESI$^+$: (m/z) calcd [M + H$^+$] for $C_{22}H_{40}ClN_4O_3Si_2$: 499.2322, found: 499.2302.

3′,5′-Di-*O*-*tert*-butyldimethylsilyl-6-cyanopurine-2′-deoxyribonucleoside (9). Nucleoside **9** was synthesized through modification to a known procedure.[12] Nucleoside **8** (0.480 g, 0.963 mmol, 1 eq.), $Zn(CN)_2$ (68.0 mg, 0.579 mmol, 0.6 eq.), and $Pd(Ph_3)_4$ (0.110 g, 0.0952 mmol, 0.1 eq.) were placed in a flame dried round bottom flask, degassed, and purged with N_2 three times and placed under N_2. Degassed anhydrous DMF (15 mL) was added to the solid mixture, heated to 90 °C and reacted for 18 hours. The reaction was diluted in DCM (50 mL), washed with H_2O (40 mL) and brine (40 mL), dried over Na_2SO_4, and concentrated *in vacuo*. The residue was purified by chromatography on silica gel with a gradient of 0–40% EtOAc in hexanes to yield **9** (0.340 g, 71% yield).

^{1}H NMR ($CDCl_3$, 500 MHz): 9.04 (s, 1H), 8.67 (s, 1H), 6.55 (app t, J = 6.3 Hz, 1H), 4.63 (app q, J = 3.8 Hz, 1H), 4.06 (app q, J = 3.2 Hz, 1H), 3.90 (dd, J = 11.4, 3.6 Hz, 1H), 3.79 (dd, J = 11.4, 2.7 Hz, 1H), 2.63 (m, 1H), 2.52 (m, 1H), 0.91 (s, 9H), 0.90 (s, 9H), 0.11 (s, 6H), 0.09 (s, 6H) δ ppm.

^{13}C NMR ($CDCl_3$, 126 MHz): 152.5, 152.2, 146.8, 135.6, 130.9, 113.6, 88.4, 85.0, 71.7, 62.6, 53.4, 41.8, 25.9, 25.7, 18.4, 18.0, −4.6, −4.8, −5.4, −5.5 δ ppm.

HRMS-ESI$^+$: (m/z) calcd [M + H$^+$] for $C_{23}H_{40}N_5O_3Si_2$: 490.2664, found: 490.2646.

6-Cyanopurine-2′-deoxyribonucleoside (1). Nucleoside **9** (388 mg, 0.792 mmol, 1 eq.) was dissolved in THF (5 mL) and to the solution was added TBAF (1.0 M in THF, 396 μL, 3.96 mmol, 5 eq.). The mixture was stirred for 15 minutes and then was concentrated *in vacuo*. The residue was purified by chromatography on silica gel with a gradient of 0–10% MeOH in DCM to yield **1** (138 mg, 0.582 mmol, 67% yield).

^{1}H NMR (DMSO-d_6, 500 MHz): 9.15 (s, 1H), 9.12 (s, 1H), 6.51 (app t, J = 6.5 Hz, 1H), 5.39 (d, J = 4.2 Hz, 1H), 4.96 (t, J = 5.4 Hz, 1H), 4.46 (m, 1H), 4.09 (app q, J = 5.3 Hz, 1H), 3.91 (app q, J = 4.1 Hz, 1H), 3.63 (m, 1H), 3.55 (m, 1H), 2.79 (m, 1H), 2.41 (m, 1H) δ ppm.

^{13}C NMR (DMSO-d_6, 126 MHz): 152.9, 152.7, 149.3, 135.9, 129.4, 114.8, 88.6, 84.7, 70.7, 61.7, 49.1 δ ppm.

HRMS-ESI$^+$: (m/z) calcd [M + H$^+$] for $C_{11}H_{12}N_5O_3$: 262.0935, found: 262.0919.

6-(Dibenzylamino)-1*H*-indole-4-carbonitrile (11). Indole **10** (50.0 mg, 0.318 mmol) was dissolved in MeOH (5.0 mL). To this solution was added K_2CO_3 (132 mg, 0.954 mmol, 3 eq.) and benzyl chloride (91.5 μL, 0.795 mmol, 2.5 eq.). The heterogeneous solution was heated to reflux for 18 hours. After cooling to room temperature, the solution was diluted with EtOAc (20 mL), washed with H_2O (10 mL, 2×) and then brine (10 mL), dried over Na_2SO_4, and concentrated *in vacuo*. The residue was purified by chromatography on silica gel with a gradient of 0–10% EtOAc in hexanes to yield **11** as a light brown solid (65.0 mg, 61% yield).

^{1}H NMR (MeOD, 500 MHz): 7.29 (m, 8H), 7.22 (m, 2H), 7.18 (d, J = 3.0 Hz, 1H), 6.99 (m, 2H), 4.67 (s, 4H) δ ppm.

^{13}C NMR (MeOD, 126 MHz): 146.3, 140.0, 139.1, 129.6, 128.1, 128.0, 126.7, 123.4, 120.2, 114.5, 102.9, 102.4, 100.3, 56.8 δ ppm.

HRMS-ESI$^+$: (m/z) calcd [M + H$^+$] for $C_{23}H_{19}N_3$: 338.1652, found: 338.1631.

(2*R*,3*S*,5*R*)-5-(4-Cyano-6-(dibenzylamino)-1*H*-indol-1-yl)-2-(((4-methylbenzoyl)oxy)methyl)tetrahydrofuran-3-yl 4-methylbenzoate (13). Nucleoside **13** was synthesized through modification to a known procedure.[19,20] **11** (250 mg, 740 μmol) was dissolved in anhydrous MeCN (10 mL). To this solution was added NaH (60% disp. oil, 39.1 mg, 1.63 mmol, 1.3 eq.) and the mixture stirred at room temperature for 30 minutes. **12** (375 mg, 960 μmol, 1.3 eq.) was added slowly with stirring. The homogeneous solution stirred for 18 hours. The solution was diluted with EtOAc (20 mL), washed with H_2O (10 mL, 2×) and then brine (10 mL), dried over Na_2SO_4, and concentrated *in vacuo*. The residue was purified by chromatography on silica gel with a gradient of 0–25% EtOAc in hexanes to yield **13** as a white solid (330 mg, 65% yield).

^{1}H NMR (MeCN-d_3, 500 MHz): 7.98 (d, J = 8.5 Hz, 2H), 7.85 (d, J = 8.5 Hz, 2H), 7.35 (d, J = 8.0 Hz, 2H), 7.30 (m, 11H), 7.22 (m, 2H), 7.10 (d, J = 2.0 Hz, 1H), 7.04 (d, J = 2.0, 1H), 6.46 (d, J = 3.5 Hz, 1H), 6.27 (dd, J = 5.5, 3.0 Hz, 1H), 5.57 (m, 1H), 4.72 (s, 4H), 4.46 (m, 3H), 2.68 (m, 1H), 2.54 (m, 1H), 2.43 (s, 3H), 2.39 (s, 3H) δ ppm.

^{13}C NMR (MeCN-d_3, 126 MHz): 166.8, 166.7, 146.0, 145.5, 145.2, 139.6, 138.5, 130.5, 130.4, 130.2, 130.2, 129.5, 128.0, 128.0, 127.9, 126.0, 123.1, 119.3, 114.8, 103.7, 101.8, 100.7, 86.1, 82.4, 75.9, 65.0, 56.4, 56.3, 37.7, 21.7, 21.6 δ ppm.

HRMS-ESI$^+$: (m/z) calcd [M + H$^+$] for $C_{44}H_{39}N_3O_5$: 690.2962, found: 690.2928.

(2*R*,3*S*,5*R*)-5-(6-Amino-4-cyano-1*H*-indol-1-yl)-2-(((4-methylbenzoyl)oxy)methyl)tetrahydrofuran-3-yl 4-methylbenzoate (14). Nucleoside **13** (1.00 g, 1.45 mmol) was added to a Parr bottle and subsequently suspended in THF (54 mL). To this suspension was added palladium on carbon (10 wt% Pd/C loading, matrix activated carbon support, 686 mg). The suspension was degassed with N_2, charged with hydrogen gas (15 psi), and shaken on a Parr Hydrogenator for 18 hours. The suspension was degassed with N_2 and filtered through a pad of Celite with THF washing (20 mL). The filtrate was concentrated *in vacuo*. The residue was purified by chromatography on silica gel with a gradient of 0–60% EtOAc in hexanes to yield **14** as a light brown solid (280 mg, 38% yield).

^{1}H NMR (MeCN-d_3, 500 MHz): 7.91 (d, J = 8.0 Hz, 2H), 7.79 (d, J = 8.0 Hz, 2H), 7.24 (m, 5H), 7.00 (s, 1H), 6.80 (s, 1H), 6.39 (d, J = 3.5 Hz, 1H), 6.29 (dd, J = 6.0, 2.5 Hz, 1H), 5.59 (d, J = 7.0 Hz, 1H), 4.50 (app q, J = 7.5 Hz, 1H), 4.43 (m, 2H), 4.15 (s, 2H), 2.75 (m, 1H), 2.60 (m, 1H), 2.34 (s, 3H), 2.32 (s, 3H) δ ppm.

^{13}C NMR (MeCN-d_3, 126 MHz): 166.9, 166.8, 145.5, 145.3, 145.0, 138.6, 130.5, 130.4, 130.4, 130.3, 130.2, 128.0, 125.7, 123.6, 119.2, 115.3, 103.8, 102.1, 101.0, 86.2, 82.5, 75.9, 65.0, 37.6, 21.6, 21.6 δ ppm.

HRMS-ESI$^+$: (m/z) calcd [M + H$^+$] for $C_{30}H_{27}N_3O_5$: 510.2023, found: 510.2017.

6-Amino-4-cyanoindole-2′-deoxyribonucleoside (2). Nucleoside **2** was synthesized through modification to a known procedure.[21] **14** (240 mg, 470 μmol) was dissolved in MeOH (5.0 mL) and CH_2Cl_2 (2.5 mL). To this solution was added K_2CO_3 (391 mg, 2.83 mmol, 6 eq.). The homogeneous solution was heated to 50 °C and stirred for 5 hours. The solution was diluted with EtOAc (20 mL), washed with H_2O (10 mL, 2×) and then brine (10 mL), dried over Na_2SO_4, and concentrated *in vacuo*. The residue was purified by chromatography on silica gel with a gradient of 0–15% MeOH in CH_2Cl_2 to yield **2** as a white solid (64.0 mg, 50% yield).

^{1}H NMR (MeOD, 500 MHz): 7.45 (d, J = 3.5 Hz, 1H), 7.16 (s, 1H), 6.94 (d, J = 1.5 Hz, 1H), 6.48 (d, J = 3.0 Hz, 1H), 6.31 (dd, J = 6.0, 2.0 Hz, 1H), 4.47 (m, 1H), 3.95 (app q, J = 3.5 Hz, 1H), 3.69 (m, 2H), 2.57 (m, 1H), 2.32 (m, 1H) δ ppm.

^{13}C NMR (MeOD, 126 MHz): 144.8, 139.0, 126.3, 124.7, 119.6, 115.8, 103.5, 102.0, 101.8, 88.3, 86.2, 72.6, 63.5, 40.9 δ ppm.

HRMS-ESI$^+$: (m/z) calcd [M + H$^+$] for $C_{14}H_{15}N_3O_3$: 274.1186, found: 274.1176.

Methyl 2-methyl-3,5-dinitrobenzoate (16). 16 was synthesized through modification to a known procedure.[22] **15** (5.00 g, 22.1 mmol) was dissolved in MeOH (80 mL). To this homogeneous solution, concentrated H_2SO_4 (5.0 mL) was added. The solution was heated to reflux for 18 hours. The flask was removed from the heat source and cooled to room temperature. The solution was concentrated *in vacuo*. The product started to precipitate out of solution upon removal of solvent. The flask was removed from the vacuum source when there was approximately 10 mL of solvent remaining and placed in an ice bath for 15 minutes to assist in precipitation. The solid was filtered with cold MeOH (30 mL) and further dried *in vacuo* to yield **16** as a white solid (5.20 g, 98% yield).

^{1}H NMR ($CDCl_3$, 500 MHz): 8.85 (d, J = 2.4 Hz, 1H), 8.69 (d, J = 2.4 Hz, 1H), 4.01 (s, 3H), 2.76 (s, 1H) δ ppm.

Methyl 6-amino-1*H*-indole-4-carboxylate (17). Indole **17** was synthesized through modification to a known procedure.[13,14] **16** (3.00 g, 12.5 mmol) was placed in a microwave vessel and dissolved in 1,4-dioxane (20 mL). To this homogeneous solution was added *N*,*N*-dimethylformamide dimethyl acetal (DMF-DMA, 2.22 mL, 1.5 eq.). The solution was subjected to microwave irradiation for 40 minutes. After cooling to room temperature another 1.5 eq. of DMF-DMA was added to the solution. It was subjected to microwave irradiation for another 40 minutes. After cooling to room temperature, the 1,4-dioxane was removed *in vacuo*. MeOH (30 mL) was added, and the solution was transferred from the microwave vessel into a round bottom flask. Pd/C (1.22 g) was slowly added to the flask with stirring. The flask was sealed with a rubber septum and purged using a vacuum line and nitrogen. Two balloons filled with H_2 gas were pierced through the septum and the solution stirred for 18 hours. The solution was filtered through 2.0 g of Celite to remove the Pd/C. The solution was then concentrated *in vacuo*. The residue was purified by chromatography on silica gel with a gradient of 0–80% EtOAc in hexanes to yield **17** as a brown solid (1.48 g, 62% yield).

^{1}H NMR (MeOD, 500 MHz): 7.36 (d, J = 2.0 Hz, 1H), 7.16 (d, J = 3.1 Hz, 1H), 7.04 (d, J = 1.1 Hz, 1H), 6.85 (d, J = 3.1 Hz, 1H), 3.92 (s, 3H) δ ppm.

Methyl 6-(dibenzylamino)-1*H*-indole-4-carboxylate (18). The procedure followed was analogous to the synthesis of **11**. The residue was purified by chromatography on silica gel with a gradient of 0–10% EtOAc in hexanes to yield **18** as a brown solid, 54% yield.

^{1}H NMR (DMSO-d_6, 500 MHz): 10.88 (s, 1H), 7.37 (d, J = 2.3 Hz, 1H), 7.32 (m, 8H), 7.24 (m, 2H), 7.21 (t, J = 2.8 Hz, 1H), 6.90 (d, J = 2.2 Hz, 1H), 6.70 (t, J = 2.6 Hz, 1H), 4.71 (s, 4H), 3.82 (s, 3H) δ ppm.

^{13}C NMR (DMSO-d_6, 126 MHz): 167.9, 144.1, 139.5, 138.7, 129.0, 127.2, 127.2, 125.6, 120.9, 119.9, 111.1, 102.2, 101.0, 55.6, 52.0 δ ppm.

HRMS-ESI$^+$: (m/z) calcd [M + H$^+$] for $C_{24}H_{23}N_2O_2$: 371.1754, found: 371.1713.

Methyl 6-(dibenzylamino)-1-((2*R*,4*S*,5*R*)-4-((4-methylbenzoyl)oxy)-5-(((4-methylbenzoyl)oxy)methyl)tetrahydrofuran-2-yl)-1*H*-indole-4-carboxylate (19). The procedure followed was analogous to the synthesis of **13**. The residue was purified by chromatography on silica gel with a gradient of 0–45% EtOAc in hexanes to yield **19** as a white solid, 64% yield.

^{1}H NMR (MeCN-d_3, 500 MHz): 8.02 (d, J = 8.0 Hz, 2H), 7.90 (d, J = 8.0 Hz, 2H), 7.47 (d, J = 2.0 Hz, 1H), 7.39 (d, J = 8.0 Hz, 2H), 7.32 (m, 10H), 7.28 (d, J = 2.0 Hz, 1H), 7.24 (t, J = 6.5 Hz, 2H), 7.11 (d, J = 2.5 Hz, 1H), 6.88 (d, J = 3.0 Hz, 1H), 6.32 (dd, J = 8.5, 5.5 Hz, 1H), 5.60 (d, J = 6.0 Hz, 1H), 4.76 (s, 4H), 4.53 (m, 1H), 4.47 (m, 2H), 3.87 (s, 3H), 2.72 (m, 1H), 2.56 (m, 1H), 2.46 (s, 3H), 2.43 (s, 3H) δ ppm.

^{13}C NMR (MeCN-d_3, 126 MHz): 168.4, 166.9, 166.7, 145.7, 145.5, 145.2, 140.3, 140.1, 130.5, 130.4, 130.2, 129.5, 128.1, 128.0, 127.9, 125.1, 122.7, 121.5, 113.1, 104.7, 103.2, 86.0, 82.3, 76.0, 65.1, 56.5, 52.2, 37.6, 21.7, 21.6 δ ppm.

HRMS-ESI$^+$: (m/z) calcd [M + H$^+$] for $C_{45}H_{42}N_2O_7$: 723.3065, found: 723.2990.

Methyl 6-amino-1-((2*R*,4*S*,5*R*)-4-((4-methylbenzoyl)oxy)-5-(((4-methylbenzoyl)oxy)methyl)tetrahydrofuran-2-yl)-1*H*-indole-4-carboxylate (20). The procedure followed was analogous to the synthesis of **14**. The residue was purified by chromatography on silica gel with a gradient of 0–50% EtOAc in hexanes to yield **20** as a brown solid, 55% yield.

^{1}H NMR (MeOD, 500 MHz): 8.00 (d, J = 10.0 Hz, 2H), 7.90 (d, J = 10.0 Hz, 2H), 7.37 (d, J = 2.0 Hz, 1H), 7.34 (d, J = 8.0 Hz, 2H), 7.31 (d, J = 3.5 Hz, 1H), 7.28 (d, J = 8.0 Hz, 2H), 7.19 (d, J = 1.5 Hz, 1H), 6.90 (d, J = 3.5 Hz, 1H), 6.47 (dd, J = 6.0, 2.5 Hz, 1H), 5.75 (m, 1H), 4.6 (m, 3H), 3.92 (s, 3H), 2.94 (m, 1H), 2.70 (m, 1H), 2.44 (s, 3H), 2.41 (s, 3H) δ ppm.

^{13}C NMR (MeOD, 126 MHz): 169.5, 167.8, 167.6, 145.8, 145.5, 143.9, 139.9, 130.8, 130.7, 130.3, 130.3, 128.2, 128.2, 125.0, 123.4, 122.8, 115.0, 105.2, 102.5, 86.6, 82.9, 76.5, 65.4, 52.2, 37.9, 21.7, 21.6 δ ppm.

HRMS-ESI$^+$: (m/z) calcd [M + H$^+$] for $C_{31}H_{30}N_2O_7$: 543.2126, found: 543.2071.

Methyl 6-amino-1-((2*R*,4*S*,5*R*)-4-hydroxy-5-(hydroxymethyl) tetrahydrofuran-2-yl)-1*H*-indole-4-carboxylate (3). The procedure followed was analogous to the synthesis of **2**. The residue was purified by chromatography on silica gel with a gradient of 0–15% MeOH in CH_2Cl_2 to yield **3** as a brown solid, 51% yield.

^{1}H NMR (MeOD, 500 MHz): 7.37 (s, 1H), 7.36 (s, 1H), 7.15 (d, J = 2.0 Hz, 1H), 6.92 (d, J = 3.5 Hz, 1H), 6.33 (dd, J = 6.5, 1.5 Hz, 1H), 4.47 (m, 1H), 3.94 (app q, J = 4.0 Hz, 1H), 3.92 (s, 3H), 3.69 (m, 2H), 2.58 (m, 1H), 2.30 (m, 1H) δ ppm.

^{13}C NMR (MeOD, 126 MHz): 169.6, 143.6, 139.8, 125.4, 123.4, 122.6, 114.8, 104.8, 102.4, 88.1, 86.0, 72.7, 63.6, 52.1, 40.7 δ ppm.

HRMS-ESI$^+$: (m/z) calcd [M + H$^+$] for $C_{15}H_{18}N_2O_5$: 307.1288, found: 307.1273.

6-Amino-1-((2*R*,4*S*,5*R*)-4-hydroxy-5-(hydroxymethyl)tetrahydrofuran-2-yl)-1*H*-indole-4-carboxylic acid (4). Nucleoside **4** was synthesized through modification to a known procedure.[23] **3** (203 mg, 663 μmol) was dissolved in THF (1.3 mL) and MeOH (1.3 mL). To this homogeneous solution was added 1.0 M aqueous KOH (3.98 mL, 3.98 mmol, 6 eq.). The solution was heated to 50 °C and stirred for 18 hours. The mixture was neutralized with 1.0 M aqueous HCl, then diluted with EtOAc (20 mL), washed with H_2O (10 mL, 2×) and then brine (10 mL), dried over Na_2SO_4, and concentrated *in vacuo*. The residue was purified by chromatography on silica gel with a gradient of 0–20% MeOH in CH_2Cl_2 to yield **4** as a brown solid (130 mg, 43% yield).

^{1}H NMR (MeOD, 500 MHz): 7.24 (d, J = 3.5 Hz, 1H), 7.20 (d, J = 2.0 Hz, 1H), 6.99 (m, 2H), 6.32 (dd, J = 6.0, 2.0 Hz, 1H), 4.46 (m, 1H), 3.92 (app q, J = 4.0 Hz, 1H), 3.67 (m, 2H), 2.59 (m, 1H), 2.28 (m, 1H) δ ppm.

^{13}C NMR (MeOD, 126 MHz): 176.9, 143.0, 139.6, 132.2, 123.5, 123.5, 113.9, 105.7, 99.5, 87.9, 86.0, 72.7, 63.7, 40.6 δ ppm.

HRMS-ESI$^+$: (m/z) calcd [M + H$^+$] for $C_{14}H_{16}N_2O_5$: 293.1132, found: 293.1130.

Methyl 1-((2*R*,4*S*,5*R*)-4-((4-methylbenzoyl)oxy)-5-(((4-methylbenzoyl)oxy)methyl)tetrahydrofuran-2-yl)-1*H*-indole-4-carboxylate (22). The procedure followed was analogous to the synthesis of **13**. The residue was purified by chromatography on silica gel with a gradient of 0–40% EtOAc in hexanes to yield **22** as a white solid, 69% yield.

^{1}H NMR (MeOD, 500 MHz): 8.01 (d, J = 8.0 Hz, 2H), 7.89 (m, 3H), 7.83 (d, J = 8.0 Hz, 1H), 7.57 (d, J = 3.0 Hz, 1H), 7.34 (d, J = 8.5 Hz, 2H), 7.28 (d, J = 8.0 Hz, 2H), 7.16 (t, J = 7.5 Hz, 1H), 7.08 (d, J = 3.0 Hz, 1H), 6.61 (dd, J = 5.5, 2.5 Hz, 1H), 5.78 (m, 1H), 4.63 (m, 3H), 3.95 (s, 3H), 2.99 (m, 1H), 2.75 (m, 1H), 2.44 (s, 3H), 2.42 (s, 3H) δ ppm.

^{13}C NMR (MeOD, 126 MHz): 169.6, 167.9, 167.8, 145.9, 145.7, 138.5, 131.0, 130.9, 130.5, 130.5, 130.4, 128.4, 128.3, 127.9, 124.8, 122.8, 122.4, 116.7, 105.4, 87.1, 83.3, 76.5, 65.4, 52.4, 38.4, 21.8, 21.8 δ ppm.

HRMS-ESI$^+$: (m/z) calcd [M + H$^+$] for $C_{31}H_{29}NO_7$: 528.2017, found: 528.1993.

Methyl 1-((2*R*,4*S*,5*R*)-4-hydroxy-5-(hydroxymethyl)tetrahydrofuran-2-yl)-1*H*-indole-4-carboxylate (5). This nucleoside has been previously prepared.[24] The procedure followed was analogous to the synthesis of **2**. The residue was purified by chromatography on silica gel with a gradient of 0–10% MeOH in CH_2Cl_2 to yield **5** as a white solid, 68% yield.

^{1}H NMR (MeOD, 500 MHz): 7.84 (d, J = 7.5 Hz, 1H), 7.82 (d, J = 8.5 Hz, 1H), 7.65 (d, J = 4.0 Hz, 1H), 7.26 (t, J = 8.0 Hz, 1H), 7.12 (d, J = 3.5 Hz, 1H), 6.49 (dd, J = 6.0, 1.5 Hz, 1H), 4.50 (m, 1H), 3.96 (m, 4H), 3.70 (m, 2H), 2.62 (m, 1H), 2.37 (m, 1H) δ ppm.

^{13}C NMR (MeOD, 126 MHz): 169.6, 138.5, 130.0, 127.9, 124.5, 122.5, 122.0, 116.1, 104.9, 88.3, 86.2, 72.7, 63.5, 52.2, 41.0 δ ppm.

HRMS-ESI$^+$: (m/z) calcd [M + H$^+$] for $C_{15}H_{17}NO_5$: 292.1179, found: 292.1173.

1-((2*R*,4*S*,5*R*)-4-Hydroxy-5-(hydroxymethyl)tetrahydrofuran-2-yl)-1*H*-indole-4-carboxylic acid (6). The procedure followed was analogous to the synthesis of **4**. The residue was purified by chromatography on silica gel with a gradient of 0–20% MeOH in CH_2Cl_2 to yield **6** as a white solid, 46% yield.

^{1}H NMR (MeOD, 500 MHz): 7.85 (d, J = 7.0 Hz, 1H), 7.78 (d, J = 8.5 Hz, 1H) 7.61 (d, J = 3.5 Hz, 1H), 7.24 (t, J = 8.0 Hz, 1H), 7.14 (d, J = 3.5 Hz, 1H), 6.48 (dd, J = 6.0, 2.0 Hz, 1H), 4.49 (m, 1H), 3.98 (app q, J = 4.0 Hz, 1H), 3.70 (m, 2H), 2.61 (m, 1H), 2.36 (m, 1H) δ ppm.

^{13}C NMR (MeOD, 126 MHz): 171.2, 138.4, 130.3, 127.6, 124.7, 123.3, 122.0, 115.8, 105.1, 88.2, 86.2, 72.7, 63.5, 41.0 δ ppm.

HRMS-ESI$^+$: (m/z) calcd [M + H$^+$] for $C_{14}H_{15}NO_5$: 278.1023, found: 278.1022.

UV absorption spectroscopy measurements

Absorbance measurements were collected on an Agilent Cary 100 UV-vis spectrometer (Simple Reads Software, spectral bandwidth 1.5 nm). Samples were dissolved in MilliQ water at 0.10 to 0.35 mM. Readings were taken at room temperature. 1 cm path length quartz cuvettes were used for all readings (1.16 mL volume, Starna Cells, Inc.).

Steady state fluorescence measurements

Steady state fluorescence measurements were collected on a Varian Cary Eclipse fluorescence spectrometer. Samples were dissolved in MilliQ water (apart from quinine sulfate in 0.105 M aq. $HClO_4$) at concentrations ranging from 0.10 to 0.35 mM. Readings were taken at room temperature with an excitation slit of 2.5 nm and an emission slit of 5.0 nm. 1 cm path length quartz cuvettes were used for all readings (1.16 mL volume, Starna Cells, Inc.).

Molar extinction coefficient determinations

A known mass of each sample was measured in a dry glass vial. To this sample was added a known volume of MilliQ water so that the concentration of each sample was known. Serial dilutions were performed so there were 6 samples of known concentration. Absorbance measurements were taken using a UV-vis at the absorbance maximum for each compound (all absorbances in the range of 0.1–1.0). 1 cm path length quartz cuvettes were used for all readings (1.16 mL volume, Starna

Cells, Inc.). Beer's law plots were constructed where the slope of the best fit line for plots of absorbance *vs.* concentration gives the molar extinction coefficient in M^{-1} cm^{-1}. This process was repeated 3 times for each sample. The molar extinction coefficients were averaged, and standard deviation was calculated using Microsoft Excel.

Quantum yield determinations

Quantum yield calculations were determined using the method described by Würth, *et al.*[18] with quinine sulfate in 0.105 M aq. $HClO_4$ used as the standard. Samples were dissolved in MilliQ water and placed in 1 cm path length quartz cuvettes (1.16 mL volume, Starna Cells, Inc.). Dilutions of the sample were performed until the absorbance measurement of the solution was near 0.05 (0.03–0.06 was considered acceptable). The absorbance of the standard (quinine sulfate dissolved in 0.105 M aq. $HClO_4$) was made to match the absorbance of the standard solution (error of 0.001 was considered acceptable). All readings were collected on an Agilent Cary 100 UV-vis spectrometer (Simple Reads Software, spectral bandwidth 1.5 nm). Fluorescence measurements were collected of the sample and the standard using the excitation wavelength of the maximum absorbance for the sample. The area under the curve of the sample and standard was calculated using the fluorometer software. All fluorescence measurements were taken using a Varian Cary Eclipse fluorescence spectrometer (excitation slit 1.5 nm, emission slit 10 nm). Quantum yield was calculated using the following equations:

$$f = 1 - 10^{-A(\lambda_{ex})} \quad (1)$$

$$F = \int_{\lambda_{ex}} I_c \lambda_{em} d\lambda_{em} \quad (2)$$

$$\Phi_{f,x} = \Phi_{f,st} \frac{F_x}{F_{st}} \frac{f_{st}}{f_x} \frac{\eta_x^2(\lambda_{em})}{\eta_{st}^2(\lambda_{em})} \quad (3)$$

where f is the absorption factor; A is the absorbance; λ_{ex} is the excitation wavelength; F is the relative integral photon flux emitted (area under the fluorescence curve); λ_{em} is the emission wavelength; Φ is the quantum yield; and η is the refractive index of the solvent. The subscript x refers to the sample and the subscript st refers to the standard. Reported quantum yields are an average of 3 replicates. Standard deviation was calculated using Microsoft Excel.

Conflicts of interest

There are no conflicts to declare.

Acknowledgements

We gratefully acknowledge funding from the National Institutes of Health P01-CA234228 and R01-GM110129. Mass spectrometry was performed at the University of Minnesota, Masonic Cancer Center, Analytical Biochemistry Core Facility, which is supported by P30-CA77598.

References

1 S. M. Law, R. Eritja, M. F. Goodman and K. J. Breslauer, *Biochemistry*, 1996, **35**, 12329–12337.
2 D. Xu, K. O. Evans and T. M. Nordlund, *Biochemistry*, 1994, **33**, 9592–9599.
3 S. P. Hancock, T. Ghane, D. Cascio, R. Rohs, R. Di Felice and R. C. Johnson, *Nucleic Acids Res.*, 2013, **41**, 6750–6760.
4 A. Dallmann, L. Dehmel, T. Peters, C. Mügge, C. Griesinger, J. Tuma and N. P. Ernsting, *Angew. Chem., Int. Ed.*, 2010, **49**, 5989–5992.
5 D. Dziuba, P. Didier, S. Ciaco, A. Barth, C. A. M. Seidel and Y. Mély, *Chem. Soc. Rev.*, 2021, **50**, 7062–7107.
6 D. Dziuba, *Methods Appl. Fluoresc.*, 2022, **10**, 044001.
7 A. A. Tanpure, M. G. Pawar and S. G. Srivatsan, *Isr. J. Chem.*, 2013, **53**, 366–378.
8 K. T. Passow and D. A. Harki, *Org. Lett.*, 2018, **20**, 4310–4313.
9 K. T. Passow, N. M. Antczak, S. J. Sturla and D. A. Harki, *Curr. Protoc. Nucleic Acid Chem.*, 2020, **80**, e101.
10 I. A. Ahmed, A. Acharyya, C. M. Eng, J. M. Rodgers, W. F. DeGrado, H. Jo and F. Gai, *Molecules*, 2019, **24**, 602–613.
11 C. Steinmetzger, C. Bäuerlein and C. Höbartner, *Angew. Chem., Int. Ed.*, 2020, **59**, 6760–6764.
12 L. L. Gundersen, *Acta Chem. Scand.*, 1996, **50**, 58–63.
13 A. Hall, S. H. Brown, I. P. Chessell, A. Chowdhury, N. M. Clayton, T. Coleman, G. M. P. Giblin, B. Hammond, M. P. Healy, M. R. Johnson, A. Metcalf, A. D. Michel, A. Naylor, R. Novelli, D. J. Spalding, J. Sweeting and L. Winyard, *Bioorg. Med. Chem. Lett.*, 2007, **17**, 916–920.
14 A. D. Batcho and W. Leimgruber, *US Pat.*, 3,976,639, 1976.
15 J. Smagowicz and K. L. Wierzchowski, *J. Lumin.*, 1974, **8**, 210–232.
16 A. Mikhaylov, S. de Reguardati, J. Pahapill, P. R. Callis, B. Kohler and A. Rebane, *Biomed. Opt. Express*, 2018, **9**, 447–452.
17 A. Albert and H. Taguchi, *J. Chem. Soc., Perkin Trans. 2*, 1973, 1101–1103.
18 C. Würth, M. Grabolle, J. Pauli, M. Spieles and U. Resch-Genger, *Nat. Protoc.*, 2013, **8**, 1535–1550.
19 N. S. Girgis, H. B. Cottam and R. K. Robins, *J. Heterocycl. Chem.*, 1988, **25**, 361–366.
20 Z. Kazimierczuk, H. B. Cottam, G. R. Revankar and R. K. Robins, *J. Am. Chem. Soc.*, 1984, **106**, 6379–6382.
21 S. S. Bag, S. K. Das and H. Gogoi, *Tetrahedron*, 2018, **74**, 2218–2229.
22 E. Fischer and A. Speier, *Chem. Ber.*, 1895, **28**, 3252–3258.
23 M. Hartmann, J. Huber, J. S. Kramer, J. Heering, L. Pietsch, H. Stark, D. Odadzic, I. Bischoff, R. Fürst, M. Schröder, M. Akutsu, A. Chaikuad, V. Dötsch, S. Knapp, R. M. Biondi, V. V. Rogov and E. Proschak, *J. Med. Chem.*, 2021, **64**, 3720–3746.
24 R. S. Coleman, Y. Dong and J. C. Arthur, *Tetrahedron Lett.*, 1993, **34**, 6867–6870.